American Mineralogist, Volume 70, pages 590–600, 1985

High-temperature structure refinements of calcite and magnesite

S. A. MARKGRAF[1] AND R. J. REEDER

Department of Earth and Space Sciences
State University of New York at Stony Brook
Stony Brook, New York 11794

Abstract

Crystal structure parameters have been determined from X-ray intensity data collected for single crystals of calcite at 24, 200, 400, 600, 750, and 800°C, and magnesite at 24, 200, 300, 400, and 500°C. Refinements utilizing a rigid-body model and an anisotropic thermal model show good agreement in thermal parameters and R values, suggesting that the rigid-body model is valid over the temperature range studied. Comparison between the two minerals' response to temperature shows markedly different behaviors of the CO_3 group. The negative thermal expansion along **a** for calcite is explained in terms of the large libration parameters and thermal expansion coefficients.

Mean thermal expansion coefficients are calculated for selected interatomic distances. A libration correction was applied to bonds within the carbonate group, and the corrected C–O interatomic distance increased more rapidly in calcite than in magnesite. Mean thermal expansion coefficients for the Ca–O interatomic distance ($\bar{\alpha}_{Ca-O} = 15.9 \times 10^{-6}°C^{-1}$) in calcite and the Mg–O distance in magnesite ($\bar{\alpha}_{Mg-O} = 15.8 \times 10^{-6}°C^{-1}$) are comparable to those found in other CaO_6 and MgO_6 octahedra.

At 800°C the l = odd reflections of calcite are unobserved preferentially ($I < 2\sigma_I$), possibly indicating the onset of orientational disorder. However, no phase transitions were found, and the decrease in intensity may be a result of increased thermal motion of the oxygen atoms.

Introduction

Much effort has been applied recently to the investigation of anion rotational disorder at high temperatures in the rhombohedral carbonates. The calcite structure consists of alternating layers of calcium cations and CO_3 groups. Within any given layer each carbonate group has the same orientation, whereas within adjacent layers each is rotated by 60° (for a recent review, see Reeder, 1983). Disordering of the two CO_3 group orientations has been suggested as an explanation for observed anomalies in experiments on calcite (cf. Carlson, 1983).

Boeke (1912) was the first investigator to report a phase transition in calcite at elevated temperatures (~985°C). Further evidence of this transition has been supplied by several workers using a variety of techniques (Chang, 1965; Cohen and Klement, 1973; Mirwald, 1976, 1979 a,b; Carlson, 1980). Mirwald, in a series of experiments, has presented evidence for another phase transition at approximately 800°C. These have been called the calcite–$CaCO_3$ IV and calcite–$CaCO_3$ V transitions at 800°C and 1000°C, respectively. In addition, Burton and Kikuchi (1984) have suggested orientational disorder in magnesite to explain the poor fit between experimental and calculated phase diagrams. Still other workers have suggested that periodic defect structures in sedimentary calcites may reflect a kind of disorder in the CO_3 sublattice (Gunderson and Wenk, 1981). However, in none of these cases has single-crystal X-ray work been undertaken in order to characterize the structure(s) in the presumed disordered state(s).

There are several interesting crystal chemical aspects of calcite and its isotypes, including the question of the variation of the C–O interatomic distance in different isotypes, geometry of the MO_6 octahedra, and an atomistic model for the different properties of the $R\bar{3}c$ carbonates. Moreover, very little is known about the effect of temperature on the calcite-type structure. An early, preliminary investigation by Tsuboi (1927) on the effect of temperature on calcite reported a marked decrease in intensity of several reflections. Tsuboi attributed this decrease to oxygen motion. In addition, an interesting structure-property relationship exists within the $R\bar{3}c$ carbonates in terms of thermal expansion. Calcite and otavite ($CdCO_3$) have negative thermal expansion of a, whereas all other $R\bar{3}c$ carbonates show positive, although quite anisotropic, thermal expansion of a and c.

In light of these questions, single crystal, high-temperature X-ray diffraction experiments were undertaken on calcite and magnesite. A preliminary account of these results has already been reported (Markgraf and Reeder, 1984).

[1] Present Address: Materials Research Laboratory, The Pennsylvania State University, University Park, PA 16802.

0003–004X/85/0506–0590$02.00

Experimental

Specimens

Calcite crystals used in this study are from Guam (Pleistocene), and are found as a coarse spar cement infilling a mollusk shell. A chemical analysis of this material by electron microprobe yielded the formula $Ca_{0.998}Mg_{0.002}CO_3$. Examination of the material with a TEM found it to be homogeneous with few dislocations. Two calcite crystals were used in the high-temperature study. The first crystal (hereafter referred to as CXL1) was a cleavage fragment with dimensions of 200 μm on a side and 85 μm thick. A second crystal (CXL2), also a clear cleavage fragment, measured approximately 150 × 100 × 100 μm. Both were examined optically and with precession photography, showing them to be single crystals having diffraction symmetry consistent with space group $R\bar{3}c$.

Magnesite crystals from the Magnesite Mine, Brumado, Brazil, were kindly donated to us by Mr. Curt Segler through Mr. Howard Belsky. An electron microprobe analysis gave the composition: $Mg_{0.984}Mn_{0.008}Fe_{0.007}Ca_{0.001}CO_3$. The material is homogeneous based on probe data and TEM investigation. A clear cleavage fragment (hereafter denoted as MAG) of approximately 100 × 100 × 50 μm was used in the high-temperature X-ray work. Optical examination showed it to be a single crystal, and Laue photography produced sharp spots.

Each crystal was mounted on a silica-glass fiber with Ceramobond 503 (Aremco Products, Inc.), placed in a 0.5 mm quartz capillary, evacuated, sealed, and placed on a standard goniometer head.

Data collection

Integrated intensity data were measured with an automated Picker four-circle diffractometer operating with graphite-monochromated Mo$K\alpha$ radiation ($\lambda = 0.7107$Å) at 24, 200, 400, 600, 750°C (CXL1); 800°C (CXL2); and 24, 200, 300, 400, 500°C (MAG). All data were collected using the ω-2θ scan mode, with a scan width of $2.0° + 0.7 \tan\theta$ and $\sigma_I/I = 0.01$, where σ_I is based on counting statistics. For CXL1 data were collected within the range $0 < 2\theta \leq 60°$, and for CXL2 and MAG, $0 < 2\theta \leq 70°$. Unit cell parameters were calculated at all temperatures at which data were collected, and at 700 (CXL1), 24 (CXL2), and 900°C (CXL2). This was accomplished by least-squares cell refinement using 24 reflections within the range $39 \leq 2\theta \leq 55°$. The exception to this was at high temperatures (800 and 900°C), where 12 reflections were used. Each reflection was centered at positive and negative 2θ, averaged, and read into the least-squares calculation. It should be noted that this technique does not quantify possible centering and orientation errors. Hence, the reported standard deviations for the lattice parameters may be low (Table 1).

Heating *in situ* was accomplished with the heater described by Brown et al. (1973). Equilibration time after each increase in temperature was roughly two hours, and the error in temperature was approximately ±20°C. A standard reflection, $04\bar{4}8$, was monitored throughout each data set; it was collected once every 20 reflections. Any large deviation in its intensity was an indication of crystal movement or decomposition. In general portions of three asymmetric units were collected at each temperature. The exception to this was at 400°C (CXL1), where the crystal was shifting; 107 independent reflections were eventually collected at this temperature.

Decomposition of the samples occurred at approximately 900°C for calcite and roughly 600°C for magnesite. The onset of decomposition was marked by the appearance of a white coating on the crystal.

Table 1. Unit cell parameters of calcite and magnesite

T(°C)	a(Å)	c(Å)	V(Å^3)
Calcite			
24*	4.988(1)**	17.061(1)	367.6(1)
200	4.984(1)	17.121(2)	368.3(1)
400	4.980(1)	17.224(2)	370.0(1)
600	4.978(3)	17.354(9)	372.4(4)
700	4.977(3)	17.425(9)	373.7(4)
750	4.978(3)	17.462(8)	374.5(3)
800	4.976(4)	17.488(12)	374.9(5)
900	4.975(2)	17.585(11)	376.9(3)
Magnesite			
24	4.635(2)	15.019(3)	279.3(2)
200	4.639(2)	15.065(3)	280.7(2)
300	4.642(2)	15.096(3)	281.6(2)
400	4.646(1)	15.139(2)	282.9(1)
500	4.650(1)	15.186(2)	284.3(1)

*CXL1 and CXL2.
**Estimated standard deviations are given in parentheses. This convention is followed in all tables.

Refinement procedures

All intensities were corrected for Lorentz and polarization factors and converted to structure factors. A reflection was considered "unobserved" when $I_{obs} < 2\sigma_I$, and was eliminated from the refinement cycles. Reflections that did not obey the rule $h\bar{h}0l$; $l = 2n$ were also collected. These reflections were deleted prior to data averaging, but not before the structure had statisfactorily refined (e.g., $R \leq 5.0\%$). An absorption correction utilizing numerical integration (L. W. Finger, unpublished) was applied to the data for CXL1 (μ(Mo$K\alpha$) = 22 cm^{-1}). The maximum and minimum of the transmission factor were 0.846 and 0.764. Because of the loss of orientation between the crystal and diffractometer, no correction was applied to CXL2. Caution should therefore be used when comparing thermal parameters between the two crystals. For magnesite, the small absorption coefficient (μ(Mo$K\alpha$) = 6 cm^{-1}) made an absorption correction unnecessary. Symmetry-averaged data were used in the final phases of refinement. Information concerning the refinements and the number of reflections collected may be found in Table 2.

The least-squares refinement program RFINE IV (Finger and

Table 2. Data collection and refinement information for calcite and magnesite

T(°C)	Total No. Obs.	No. Indep. Obs.	Rw*	R**	S***
Calcite					
24	412	113	0.029	0.022	2.91
200	328	117	0.026	0.020	2.30
400	521	107	0.055	0.049	2.24
600	223	112	0.063	0.055	4.41
750	333	100	0.063	0.050	4.97
800	517	148	0.063	0.059	3.91
Magnesite					
24	391	139	0.034	0.030	2.97
200	391	138	0.033	0.026	2.21
300	391	137	0.032	0.025	2.60
400	393	139	0.034	0.027	2.69
500	391	136	0.037	0.032	2.88

*Rw = $[\Sigma w(|F_O|-|F_C|)^2/\Sigma w|F_O|^2]^{\frac{1}{2}}$.
**R = $(\Sigma||F_O|-|F_C||)/\Sigma|F_O|$.
***S = Standard deviation of an observation of unit weight.

Prince, 1975) was used in all structure refinements. A weighting scheme of $1/\sigma_F^2$, with σ_F based on counting statistics, was used. Starting parameters for the calcite and magnesite room-temperature refinements were taken from Effenberger et al. (1981). At higher temperatures the parameters determined at the previous temperature refinement were used as starting values. Variable parameters consisted of an overall scale factor, the x positional coordinate of oxygen and its four independent anisotropic temperature factors, and two independent anisotropic thermal parameters each for carbon and calcium. Atomic scattering factor curves for neutral atoms were taken from the *International Tables for X-Ray Crystallography, Vol. IV* (1974), as were corrections for anomalous dispersion. The extinction correction of Zachariasen (1967) was applied to CXL1, but not CXL2 or MAG. We repeated the refinements of CXL1 at 24 and 750°C using a modified version of RFINE IV incorporating the isotropic extinction correction of Becker and Coppens (1975), assuming Type I (Lorentzian) behavior. There was no significant difference in thermal parameters within the standard errors calculated. An extinction coefficient (Zachariasen model) of 0.3988×10^{-4} was calculated for CXL1, 24°C. The **TLS** refinements (see below) gave results similar to the anisotropic refinements, and a trend in which r* decreases with increasing temperature was noted.

Rigid-body refinements, utilizing the three tensors **T**, **L**, and **S** to describe the average thermal motion of a rigid body (Schomaker and Trueblood, 1968) were carried out for the carbonate group in calcite and magnesite. Finger (1975) has previously analyzed calcite and magnesite in this manner at room temperature, and has correlated the results with vibrational frequencies. Starting parameters for the rigid-body tensors were taken from his study, and symmetry-averaged data were used.

Results

Unit cell parameters (a, c, volume) are given in Table 1, and shown in Figures 1 and 2. Anisotropic refinements resulted in unweighted R factors ranging from 0.022 (CXL1, 24°C) to 0.059 (CXL2, 800°C) for calcite and 0.030 (24°C) to 0.032 (500°C) for magnesite. See Table 2 for a listing of R factors for the anisotropic refinements. **TLS** parameters derived from the rigid-body refinements, along with the residuals, are given in Table 3.

The x positional parameter for oxygen and the anisotropic temperature factors for calcite and magnesite at all temperatures are given in Table 4. Both anisotropic and **TLS** refinement results are reported. It is interesting to note that the x coordinate in magnesite decreases even after a correction for libration has been applied. Final observed and calculated structure factors for all data sets are tabulated in Table 5.[2]

Thermal parameters

The equivalent isotropic temperature factors B_{eq} are the same for the anisotropic and rigid-body refinements. Figure 3 shows B_{eq} vs. temperature for the anisotropic refinements. The slopes of B_{eq} vs. temperature for the carbon and oxygen atoms in magnesite are similar. It seems probable that some correlation in thermal motion exists between them. The riding model of Busing and Levy (1964), applied to the isostructural $NaNO_3$ by Cherin et al. (1967), may be applicable in magnesite over the temperature range studied. In contrast the carbon and oxygen of calcite show poor correlation with the B_{eq} for the O atom increasing

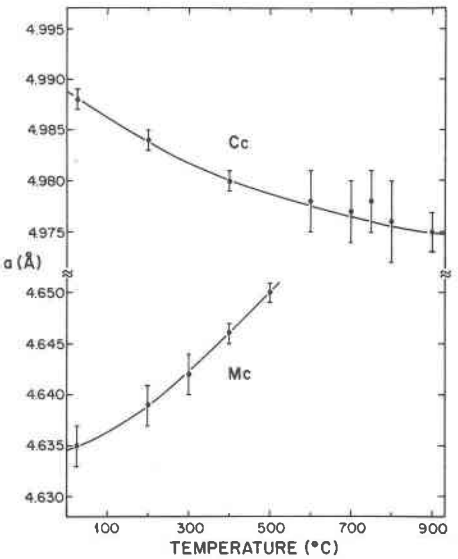

Fig. 1. Variation of a unit cell parameter with increasing temperature for calcite and magnesite. (Error bars represent 2 standard deviations; if no error bar is given 2 standard deviations are contained within the area of the symbol. Abbreviations: Cc = calcite, Mc = magnesite. These conventions are followed in all Figures.)

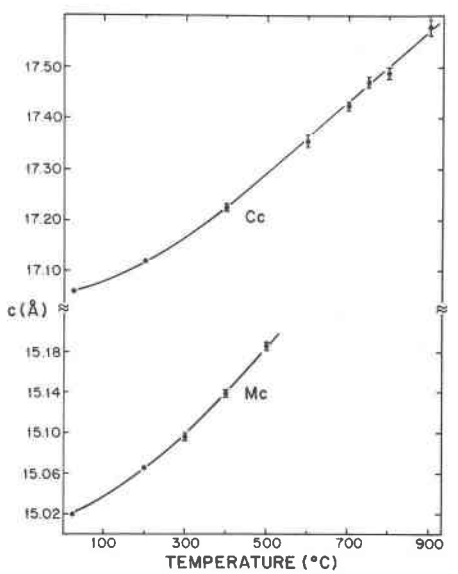

Fig. 2. Variation of c unit cell parameter with increasing temperature for calcite and magnesite.

[2] To receive a copy of Table 5, order Document AM-85-267 from the Business Office, Mineralogical Society of America, 2000 Florida Avenue, N.W., Washington, D. C. 20009. Please remit $5.00 in advance for the microfiche.

Table 3. Rigid-body parameters and residuals for calcite and magnesite

Temp. (°C)	T_{11} (Å^2)	T_{33} (Å^2)	L_{11} (RAD^2)	L_{33} (RAD^2)	S_{11} (RAD^2)	R	Rw
Calcite							
24	0.0104(7)	0.013(2)	0.006(1)	0.0084(6)	0.0022(2)	0.022	0.029
200	0.035(6)	0.018(1)	0.009(1)	0.0134(6)	0.0033(2)	0.021	0.027
400	0.021(1)	0.036(5)	0.016(4)	0.020(2)	0.005(1)	0.050	0.055
600	0.030(2)	0.034(3)	0.025(2)	0.026(2)	0.008(2)	0.057	0.066
750	0.036(2)	0.040(4)	0.032(3)	0.041(4)	0.010(2)	0.052	0.066
800	0.036(1)	0.049(3)	0.027(3)	0.054(3)	0.011(2)	0.058	0.063
Magnesite							
24	0.0045(3)	0.0065(7)	0.0016(4)	0.0017(3)	0.0002(1)	0.032	0.036
200	0.0061(3)	0.0083(7)	0.0025(5)	0.0022(2)	0.0004(2)	0.028	0.035
300	0.0073(3)	0.0097(7)	0.0032(4)	0.0027(2)	0.0005(2)	0.028	0.034
400	0.0090(3)	0.0112(7)	0.0044(5)	0.0032(3)	0.0006(2)	0.028	0.035
500	0.0101(4)	0.0147(8)	0.0053(5)	0.0038(3)	0.0007(2)	0.033	0.039

quickly. Possible explanations for the poor correlation include marked anharmonicity and systematic errors.

In the high-temperature study of pyroxenes by Cameron et al. (1973) a trend was observed in which cations with low charge and high coordination have increased equivalent isotropic temperature factors relative to high charge/low coordination cations. Tremolite also shows this (Sueno et al., 1973). Within calcite and magnesite we find the same relationship: C, representing a high charge/low coordination ion, has a smaller slope than either metal (low charge/high coordination) ion. The pyroxene data also show that the slope of the B_{eq} vs. temperature line is di-

Table 4. Positional parameters and anisotropic temperature factors* (Å^2) for calcite and magnesite

Temp. (°C)	Atom	Anisotropic refinement x_{oxygen}	β_{11}*	β_{22}	β_{33}	β_{23}	Rigid-body refinement x_{oxygen}**	β_{11}	β_{22}	β_{33}	β_{23}
Calcite											
24	C		0.012(1)		0.0008(1)			0.0110(7)		0.0009(1)	
	Ca		0.0122(5)		0.00085(3)			0.1236(5)		0.00086(3)	
	O	0.2567(2)	0.0142(7)	0.0256(8)	0.00159(5)	-0.0022(1)	0.2586(3)	0.0147(6)	0.0256(8)	0.00159(5)	-0.0022(2)
200	C		0.0159(9)		0.00101(9)			0.0143(7)		0.00119(9)	
	Ca		0.0171(4)		0.00111(3)			0.0173(4)		0.00113(3)	
	O	0.2562(2)	0.0195(6)	0.0376(7)	0.00221(4)	-0.0033(1)	0.2590(3)	0.0203(5)	0.0376(8)	0.00221(4)	-0.0034(2)
400	C		0.023(2)		0.0022(4)			0.022(1)		0.0024(3)	
	Ca		0.0269(7)		0.0023(1)			0.0271(7)		0.0024(1)	
	O	0.2558(5)	0.031(1)	0.058(2)	0.0041(2)	-0.0051(5)	0.2604(5)	0.031(1)	0.057(2)	0.0041(2)	-0.0051(5)
600	C		0.0356(2)		0.0021(2)			0.033(2)		0.0022(2)	
	Ca		0.0382(9)		0.00243(6)			0.0387(9)		0.00245(6)	
	O	0.2547(8)	0.043(2)	0.079(3)	0.0050(2)	-0.0079(7)	0.2609(8)	0.045(1)	0.079(4)	0.0050(2)	-0.2609(8)
750	C		0.042(2)		0.0023(2)			0.038(2)		0.0026(2)	
	Ca		0.0464(9)		0.00306(7)			0.0467(10)		0.00308(8)	
	O	0.2528(10)	0.055(2)	0.110(5)	0.0060(2)	-0.0099(9)	0.2622(11)	0.057(2)	0.108(5)	0.0059(2)	-0.0097(9)
800	C		0.039(2)		0.0032(2)			0.039(1)		0.0032(2)	
	Ca		0.0512(7)		0.0299(5)			0.0514(7)		0.00300(5)	
	O	0.2530(9)	0.063(2)	0.131(5)	0.0061(2)	-0.0113(9)	0.2635(9)	0.064(1)	0.131(4)	0.0061(2)	-0.1013(9)
Magnesite											
24	C		0.0071(5)		0.0005(1)			0.0056(4)		0.00057(7)	
	O	0.2778(2)	0.0058(4)	0.0091(4)	0.00082(4)	-0.0003(1)	0.2782(2)	0.0064(4)	0.0090(5)	0.00080(4)	-0.0003(1)
	Mg		0.0059(3)		0.00056(3)			0.0059(3)		0.00059(3)	
200	C		0.0089(5)		0.00065(6)			0.0075(4)		0.00072(6)	
	O	0.2775(2)	0.0081(4)	0.0121(4)	0.00109(4)	-0.0004(1)	0.2781(2)	0.0086(4)	0.0120(5)	0.00108(4)	-0.0005(1)
	Mg		0.0087(3)		0.00080(3)			0.0027(3)		0.00081(3)	
300	C		0.0104(5)		0.00076(6)			0.0089(4)		0.00084(6)	
	O	0.2772(2)	0.0097(4)	0.0144(4)	0.00132(3)	-0.0006(1)	0.2780(2)	0.0103(4)	0.0143(5)	0.00130(4)	-0.0006(1)
	Mg		0.0107(3)		0.00099(3)			0.0107(3)		0.00100(3)	
400	C		0.0121(5)		0.00090(6)			0.0110(4)		0.00096(6)	
	O	0.2767(2)	0.0122(4)	0.0175(5)	0.00160(4)	-0.0007(1)	0.2778(2)	0.0126(4)	0.0174(5)	0.00158(4)	-0.0007(1)
	Mg		0.0134(3)		0.00120(3)			0.0134(3)		0.00120(3)	
500	C		0.01360(6)		0.00118(7)			0.0123(5)		0.00125(7)	
	O	0.2764(2)	0 0138(4)	0.0202(6)	0.00202(5)	-0.0008(1)	0.2777(2)	0.0143(4)	0.0201(6)	0.00200(5)	-0.0008(1)
	Mg		0.0158(4)		0.00154(2)			0.0158(4)		0.00154(4)	

*Anisotropic temperature of the form: $\exp\{-(\beta_{11}h^2+\beta_{22}k^2+\beta_{33}\ell^2+2\beta_{12}hk+2\beta_{13}h\ell+2\beta_{23}k\ell)\}$.
**Corrected for libration.

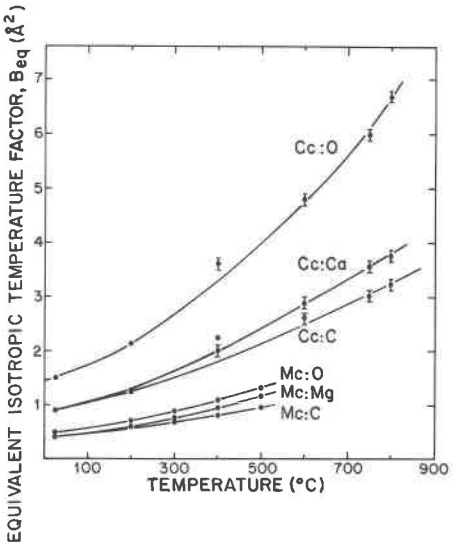

Fig. 3. Variation of the equivalent isotropic temperature factor (B_{eq}) with increasing temperature for calcite and magnesite.

rectly proportional to the M–O distance. This is similar to the results for calcite and magnesite; calcite, with the larger M–O interatomic distance also has the greater metal B_{eq} vs. temperature slope.

The room temperature root-mean-square (RMS) displacements obtained for magnesite and calcite are in good agreement with those reported by other workers (cf. Reeder, 1983). Table 6 gives the RMS amplitudes calculated from BONDAN (Finger and Prince, 1975) for both anisotropic and rigid-body refinements at all temperatures studied. Agreement between the two types of refinements is very good. Thermal ellipsoids for the M^{2+} and C ions are constrained by the point symmetry to be ellipsoids of revolution, and for oxygen, the ellipsoid must have one of its principal axes along the C–O bond. This is the shortest RMS amplitude for oxygen. The oxygen atom, anisotropic at room temperature due to the variability of the bonds surrounding it, remains anisotropic in both minerals at all temperatures. Carbon remains approximately spherical throughout the temperature range studied, as does calcium. Magnesium becomes slightly prolate at higher temperatures. In addition, the angle R_3 (for oxygen) shows little

Table 6. Magnitudes (Å) and orientations of the principal axes of thermal ellipsoids in calcite and magnesite

Temp. (°C)	Atom	Anisotropic refinement R_1	R_2	R_3	α*(°)	Rigid-body refinement R_1	R_2	R_3	α*(°)
Calcite									
24	C	0.107(5)		0.111(7)		0.102(5)		0.115(7)	
	Ca	0.108(2)		0.112(2)		0.108(1)		0.112(2)	
	O	0.099(4)	0.125(3)	0.179(2)	46(2)	0.102(2)	0.124(3)	0.180(2)	46(2)
200	C	0.123(1)		0.128(5)		0.1164(7)		0.133(5)	
	Ca	0.127(1)		0.128(2)		0.128(1)		0.129(2)	
	O	0.113(3)	0.147(2)	0.216(2)	48(1)	0.117(1)	0.147(2)	0.216(2)	48(1)
400	C	0.148(4)		0.181(15)		0.144(4)		0.189(14)	
	Ca	0.159(1)		0.187(4)		0.160(1)		0.188(4)	
	O	0.142(5)	0.196(5)	0.278(5)	39(2)	0.146(5)	0.196(5)	0.278(5)	40(2)
600	C	0.179(8)		0.183(4)		0.177(3)		0.184(8)	
	Ca	0.190(2)		0.192(3)		0.191(1)		0.193(3)	
	O	0.172(6)	0.214(6)	0.324(6)	44(2)	0.180(6)	0.213(6)	0.323(6)	44(2)
750	C	0.190(4)		0.198(4)		0.190(5)		0.199(9)	
	Ca	0.209(2)		0.217(3)		0.210(2)		0.218(3)	
	O	0.186(5)	0.245(6)	0.369(8)	49(2)	0.196(5)	0.243(6)	0.365(8)	49(2)
800	C	0.191(3)		0.222(7)		0.191(3)		0.222(7)	
	Ca	0.215(2)		0.220(1)		0.215(2)		0.220(1)	
	O	0.197(4)	0.251(5)	0.392(7)	54(2)	0.199(4)	0.251(5)	0.392(7)	54(2)
Magnesite									
24	Mg	0.070(5)		0.081(2)		0.069(3)		0.082(2)	
	C	0.075(5)		0.076(2)		0.067(2)		0.081(5)	
	O	0.062(3)	0.084(2)	0.099(2)	22(5)	0.067(3)	0.083(2)	0.098(2)	23(5)
200	Mg	0.085(2)		0.096(2)		0.084(1)		0.096(2)	
	C	0.086(4)		0.086(4)		0.078(2)		0.091(4)	
	O	0.074(2)	0.097(2)	0.115(2)	23(4)	0.078(2)	0.096(2)	0.114(2)	24(4)
300	Mg	0.093(1)		0.107(2)		0.093(1)		0.107(2)	
	C	0.092(1)		0.094(4)		0.086(2)		0.098(4)	
	O	0.082(2)	0.105(2)	0.127(2)	23(3)	0.086(2)	0.105(2)	0.126(2)	24(3)
400	Mg	0.105(1)		0.118(2)		0.105(1)		0.118(2)	
	C	0.140(2)		0.102(4)		0.095(2)		0.106(3)	
	O	0.092(2)	0.116(2)	0.140(2)	23(2)	0.095(2)	0.115(2)	0.139(2)	24(2)
500	Mg	0.114(1)		0.134(2)		0.114(1)		0.134(2)	
	C	0.106(1)		0.118(4)		0.101(1)		0.121(4)	
	O	0.098(2)	0.127(2)	0.158(2)	18(2)	0.101(2)	0.125(2)	0.156(2)	18(2)

*α is the angle R_3 makes with c.

Table 7. Selected interatomic distances (Å) for calcite and magnesite

Temp. (°C)	M-O	O(1)-O(2)	O(1)-O(6)	C-O	C-O*	$(O-O)_{CO_3}$	$(O-O)_{CO_3}$*
Calcite							
24	2.3595(5)	3.262(1)	3.4105(4)	1.280(1)	1.2901(5)	2.218(2)	2.2345(9)
200	2.3628(5)	3.262(1)	3.4190(4)	1.277(1)	1.2916(5)	2.211(2)	2.2371(9)
400	2.368(1)	3.261(3)	3.4331(9)	1.274(3)	1.298(1)	2.206(4)	2.247(2)
600	2.376(2)	3.266(5)	3.453(2)	1.268(4)	1.301(2)	2.196(7)	2.254(3)
750	2.387(3)	3.277(6)	3.471(2)	1.258(5)	1.305(3)	2.179(9)	2.261(5)
800	2.387(3)	3.274(5)	3.474(2)	1.259(4)	1.312(2)	2.181(7)	2.272(4)
Magnesite							
24	2.1018(4)	2.925(1)	3.0195(3)	1.288(1)	1.289(1)	2.230(1)	2.233(1)
200	2.1060(4)	2.929(1)	3.0271(3)	1.287(1)	1.290(1)	2.229(1)	2.234(1)
300	2.1090(4)	2.932(1)	3.0324(3)	1.287(1)	1.290(1)	2.229(1)	2.235(1)
400	2.1134(4)	2.937(1)	3.0399(3)	1.286(1)	1.291(1)	2.227(1)	2.235(1)
500	2.1176(5)	2.941(1)	3.0477(3)	1.285(1)	1.291(1)	2.227(2)	2.236(2)

*Libration correction applied.

change with temperature in either calcite or magnesite (Table 6).

Bond lengths and angles vs. temperature

Libration causes an apparent decrease of the C–O interatomic distance. This is due to the electron density being smeared out along an arc, and leads to a bond-length correction applicable to interatomic distances affected by libration. The program BONDAN (Finger and Prince, 1975) utilizes the libration parameters from the rigid-body refinements to calculate the correction as $\delta\ r(\alpha) = r(\alpha)(L_{11} + L_{33})/2$, where $r(\alpha)$ is the interatomic distance and L_{11} and L_{33} are the mean-square amplitudes of libration about the **a** and **c** axes, respectively (Willis and Pryor, 1975, p. 197).

Interatomic distances for C–O and $(O–O)CO_3$, both corrected and uncorrected, are given in Table 7. Figures 4 and 5 compare corrected and uncorrected bond-lengths for C–O and $(O–O)CO_3$. The sharp decrease in the uncorrected bond lengths in calcite is an indication of increased thermal motion, specifically libration. This is in contrast to the slight motion of magnesite. It is interesting to note that although the riding model of Busing and Levy (1964) is not strictly applicable when the motion involved is curvilinear (rather than rectilinear), this correction gives the same result as the libration correction. This is due to the relatively small (in comparison to some organic compounds) rigid-body motion of the carbonate group within the temperature range studied.

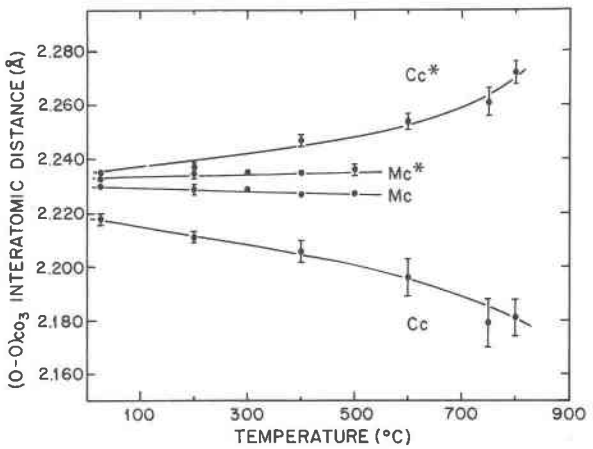

Fig. 5. Variation of the $(O–O)_{CO_3}$ interatomic distance with increasing temperature for calcite and magnesite. Abbreviations are the same as those used in Figure 4.

Octahedral bond lengths are given in Table 7 for both calcite and magnesite as a function of temperature. The metal–oxygen interatomic distances vs. temperature are shown in Figure 6. Octahedral volume vs. temperature, along with quadratic elongation (Robinson et al., 1971), are listed in Table 8. Both CaO_6 and MgO_6 octahedra become more distorted with increasing temperature.

The O(1)–M–O(2) bond angle decreases in both minerals with increasing temperature (Table 9), and the O(1)–M–O(6) increases (oxygen atoms are labelled according to the convention described in Reeder, 1983). However, the changes are not large. M–O–M angles are listed in Table 9.

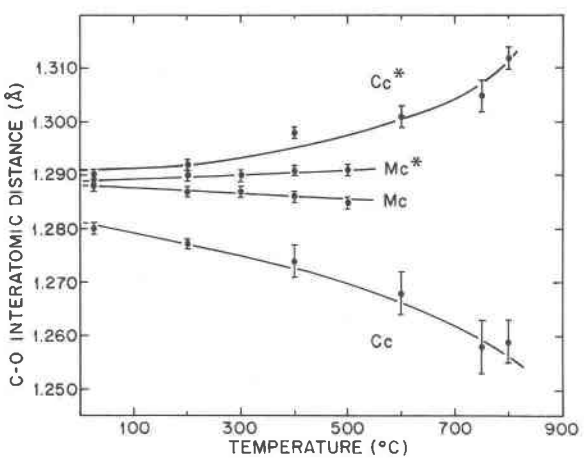

Fig. 4. Variation of the C–O interatomic distance with increasing temperature for calcite and magnesite. Abbreviations: Cc* = calcite, corrected for libration, Cc = calcite, uncorrected. The same labelling scheme is used for magnesite (Mc).

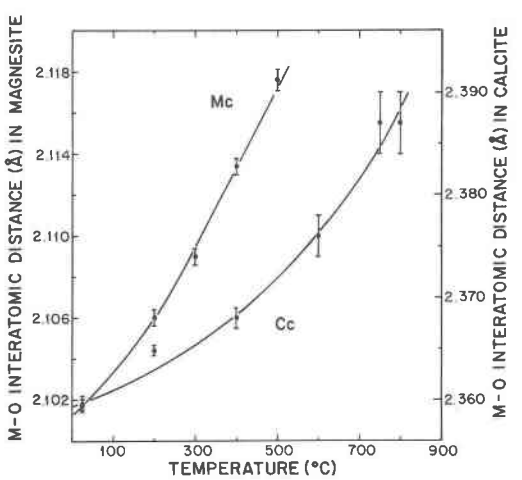

Fig. 6. Variation of the M–O interatomic distance with increasing temperature for calcite and magnesite.

Table 8. Octahedral volume (Å^3) and quadratic elongation (QE) for calcite and magnesite

Temp. (°C)	V, Å^3	QE
Calcite		
24	17.43	1.0019
200	17.53	1.0021
400	17.63	1.0026
600	17.81	1.0030
750	18.04	1.0032
800	18.04	1.0034
Magnesite		
24	12.36	1.0010
200	12.43	1.0011
300	12.47	1.0011
400	12.56	1.0012
500	12.64	1.0012

Discussion

Thermal expansion coefficients have been tabulated with a mean (linear) thermal expansion coefficient (MTEC), defined as:

$$\text{MTEC} \simeq \bar{\alpha}_X = \frac{1}{X_{24}}\left(\frac{X_T - X_{24}}{T - 24}\right);$$

where X_{24} is the room temperature value of the parameter in question and $(X_T - X_{24})/(T - 24)$ is the slope determined from a linear regression of X vs. T. Strictly speaking, a mean linear expansion coefficient is not appropriate since several of the relationships observed deviate significantly from linearity. Nevertheless, we report MTEC's as an approximate measure of thermal expansion for comparison with other structures. MTEC's for cell parameters and interatomic distances are given in Table 10.

Coefficients of thermal expansion for calcite, obtained by a variety of methods, have been reviewed by Rao et al. (1968). Our values show a marked deviation from theirs ($\bar{\alpha}_a = -3.7 \times 10^{-6}°C^{-1}$; $\bar{\alpha}_c = 25.6 \times 10^{-6}°C^{-1}$). Our larger values can be explained satisfactorily by consideration of the increased temperature range of the present study, and the nonlinearity of our data. Rao et al. (1968) measured cell parameters up to 524°C, whereas we present data to 900°C. At higher temperatures the negative thermal expansion of a becomes less negative, as observed by Mirwald (1979b). It does not become positive within the temperature range of the present study. This will have the net effect of increasing the MTEC of a, hence giving a larger value. In a similar fashion, Rao has observed that $\bar{\alpha}_c$ becomes larger at higher temperatures.

Our MTEC's for the cell edges of magnesite agree well with those reported by Bayer (1971) ($\bar{\alpha}_a = 5.5 \times 10^{-6}°C^{-1}$; $\bar{\alpha}_c = 21.0 \times 10^{-6}°C^{-1}$). Bayer's values were determined over a temperature range similar to ours.

MTEC's for the cation–oxygen interatomic distance, along with the expansion coefficients for the O–O bonds outlining the octahedra, are given in Table 10. Our metal–oxygen MTEC's are similar to Mg–O and Ca–O (octahedrally coordinated) expansion coefficients of different structures:

$\bar{\alpha}_{Mg-O} = 12.4 \times 10^{-6}°C^{-1}$ in MgO (Hazen, 1976)

$\bar{\alpha}_{Mg-O} = 14.4 \times 10^{-6}°C^{-1}$ in $CaMgSi_2O_6$ (Cameron et al., 1973)

$\bar{\alpha}_{Mg-O} = 15.8 \times 10^{-6}°C^{-1}$ in $MgCO_3$ (present study)

$\bar{\alpha}_{Mg-O} = 12.4 \times 10^{-6}°C^{-1}$ in $CaMgSiO_4$ (Lager and Meagher, 1978)

$\bar{\alpha}_{Ca-O} = 13.0 \times 10^{-6}°C^{-1}$ in CaO (Beals and Cook, 1957)

$\bar{\alpha}_{Ca-O} = 13.2 \times 10^{-6}°C^{-1}$ in $CaMgSiO_4$ (Lager and Meagher, 1978)

$\bar{\alpha}_{Ca-O} = 15.9 \times 10^{-6}°C^{-1}$ in $CaCO_3$ (present study)

The observations, along with those for octahedral volume, agree with the observation made by Hazen and Prewitt (1972) and Hazen and Finger (1982, p. 136) that a coordination polyhedron of a certain cation has similar thermal expansion behavior in a variety of different linkages. Although this observation was previously applied to oxides and silicates, it appears that rhombohedral carbonates may also be included.

Table 9. Selected bond angles (°) for calcite and magnesite

Temp. (°C)	O(1)-M-O(2)		O(1)-M-O(6)		M-O-M	
	Anisotropic	Rigid-body	Anisotropic	Rigid-body	Anisotropic	Rigid-body
Calcite						
24	87.44(1)	87.31(2)	92.56(1)	92.69(3)	85.98(2)	85.97(2)
200	87.31(1)	87.10(2)	92.69(1)	92.90(1)	86.12(3)	86.10(3)
400	87.06(3)	86.74(5)	92.94(3)	93.26(6)	86.33(6)	86.31(6)
600	86.82(6)	86.36(9)	93.18(6)	93.64(11)	86.58(11)	86.55(11)
750	86.70(7)	86.05(12)	93.30(7)	93.95(14)	86.78(14)	86.74(14)
800	86.61(6)	85.47(9)	93.39(6)	94.03(11)	86.84(11)	86.73(11)
Magnesite						
24	88.17(1)	88.15(1)	91.83(1)	91.85(1)	84.17(1)	84.17(1)
200	88.11(1)	88.07(1)	91.89(1)	91.93(1)	84.24(1)	84.23(1)
300	88.07(1)	88.02(1)	91.93(1)	91.98(1)	84.28(1)	84.27(1)
400	88.02(1)	87.95(1)	91.98(1)	92.05(1)	84.35(1)	84.34(1)
500	87.95(1)	87.87(1)	92.05(1)	92.13(1)	84.43(1)	84.40(1)

Table 10. Mean thermal expansion coefficients ($10^{-6}°C^{-1}$) in calcite and magnesite

	Calcite	Magnesite
a	-2.8	6.75
c	32.3	22.9
M-O	15.9	15.8
O(1)-O(2)	5.7	11.5
O(1)-O(6)	25.1	19.3
C-O	-22.6	-4.6
C-O*	19.8	3.4
$(O\text{-}O)_{CO_3}$	-22.7	-3.1
$(O\text{-}O)_{CO_3}$*	20.0	2.7

*Corrected for libration.

The carbonate group

We now turn our attention to the carbonate group. The CO_3 group in the $R\bar{3}c$ carbonates is a structural unit with point group symmetry 32. Table 11 gives the C–O interatomic distances at room temperature for the known carbonate isotypes of calcite; it also lists the uncorrected values and corrected bond lengths from the present study. Effenberger et al. (1981) applied a riding model correction to the C–O interatomic distance in the $R\bar{3}c$ carbonates. We have pointed out previously that this type of correction gives results identical to a libration correction. The most striking features are the almost constant C–O value (Effenberger et al., 1981) and the lower variance in comparison to the raw values.

It is common when considering the $R\bar{3}c$ carbonates to ignore the carbonate group, considering it to behave identically in all isotypes. Certainly the C–O interatomic distances are very similar, but examination of the polarizability (Lo, 1973; Isherwood and James, 1976) or thermal parameters, two quantities that depend greatly on crystalline environment, show differences from mineral to mineral. In terms of temperature, we may further investigate this feature by examining the respective MTEC's for the C–O and $(O\text{–}O)_{CO_3}$ interatomic distance, along with the rigid-body parameters for each mineral.

Comparison of the thermal parameters derived from the anisotropic refinements and from the rigid body model shows excellent agreement (Tables 4 and 7), and the R factors for the rigid-body refinements are comparable to the anisotropic model (it should be noted that the rigid-body refinement contains one less variable). This strongly suggests that the rigid-body model is applicable to calcite and magnesite. Internal modes, which a standard rigid-body model like ours does not account for, are assumed to be unimportant. In calcite this assumption is supported by the high-temperature Raman spectra work of Narayanaswamy (1947). It is this assumption that gives the model its physical significance, for with a conventional Bragg scattering type of experiment we cannot distinguish between rigid-body motion and activation of internal modes (Willis and Pryor, 1975, p. 187).

The MTEC's for the corrected C–O and $(O\text{–}O)_{CO_3}$ interatomic distances are given in Table 10. The approximate agreement between the MTEC's for C–O and $(O\text{–}O)_{CO_3}$ for each group is further evidence of rigid-body behavior. The MTEC for the C–O interatomic distance in calcite is roughly five times that of magnesite, whereas the MTEC for $(O\text{–}O)_{CO_3}$ is approximately six times greater in calcite. Certainly the two carbonate groups are behaving differently (if only in magnitude), with the carbonate member in calcite undergoing greater thermal deformation.

The conclusion drawn from the MTEC's for the carbonate group, that the CO_3 group in calcite undergoes greater thermal expansion than in magnesite, is further supported through examination of **TLS** parameters. Five independent **TLS** parameters are refined for the CO_3 group in a calcite structure type. They are: T_{11} $(=T_{22})$, describing the translation within the plane normal to **c**; T_{33}, for translations parallel to **c**; L_{11} $(=L_{22})$, for librations about the axes normal to **c**; L_{33} for libration about the unique axis; and S_{11}, the parameter describing screw motion (coupled libration and translation of the group). There are two ways to derive the rigid-body parameters: (1) by first calculating the anisotropic temperature factors and then computing the **TLS** parameters; and (2) refining the structural parameters directly to obtain **T**, **L**, and **S** values (Willis and Pryor, 1975, p. 186). It is the latter method that we have used (Finger and Prince, 1975).

Overall, the rigid-body parameters are larger in calcite than in magnesite. They also increase faster, that is, respond more to temperature than those of magnesite. The trend $T_{11} < T_{33}$ is observed in both minerals (Table 3). In calcite $L_{11} < L_{33}$, while in magnesite it is just the opposite, $L_{11} > L_{33}$. The **S** parameter is an order of magnitude larger in calcite than in magnesite. It is the ten-fold differnce in the L_{11} and L_{33} parameters *between* minerals that expresses itself in the small correction to the C–O interatomic distance in magnesite and the larger one in calcite.

Our data indicate that the dominant motion in calcite is libration, whereas in magnesite it is translation. Several

Table 11. Room temperature C–O interatomic distances (Å) in $R\bar{3}c$ carbonates: uncorrected and corrected values

	Uncorrected	Corrected
$FeCO_3$*	1.2859(5)	1.2895
$ZnCO_3$*	1.2859(6)	1.2881
$MnCO_3$*	1.2867(5)	1.2898
$MgCO_3$*	1.2852(4)	1.2873
$CaCO_3$*	1.2815(6)	1.290
$MgCO_3$**	1.288(1)	1.289(1)
$CaCO_3$**	1.281(1)	1.290(1)

*Effenberger et al. (1981), riding model of Busing and Levy (1964).
**This study, libration correction.

investigators have concluded that the CO_3 group in calcite undergoes a screw-like motion (Megaw, 1970; Peterson et al., 1979). The large S_{11} parameter we have obtained supports this hypothesis. Of course, any translation combined with a libration may be defined as screw-like motion. Megaw's hypothesis that the CO_3 group in calcite undergoes rotation within the plane and translation perpendicular to that plane is supported by the large T_{33} and L_{33} parameters in Table 3. In contrast, through examination of the T_{33} and L_{11} coefficients, it is possible to describe the carbonate motion in magnesite as rotation out of the plane and translation along the three-fold axis. This speaks only of the dominant modes, using a rigid-body model, and does not preclude other forms of motion being possible.

Thermal expansion

Calcite-type structures may be approximated as filled octahedra sharing corners (Megaw, 1970). In corner-linked structures, such as calcite, there are two mechanisms active in explaining the thermal expansion: expansion of the polyhedra and tilting (or opening) of the structure (Megaw, 1973). For magnesite and calcite, the structures open slightly with increased temperature, as evidenced by the change in the M-O-M bond angle: $\sim 0.1°/100°C$ in calcite and $\sim 0.07°/100°C$ in magnesite (Table 9). MTEC's for the octahedral volume in calcite and magnesite are $47.2 \times 10^{-6}°C^{-1}$ and $46.9 \times 10^{-6}°C^{-1}$, respectively. The value for the MgO_6 agrees well with values reported for similar MgO_6 octahedra (cf. Hazen and Finger, 1982). Few high-temperature data have been reported for Ca in octahedral coordination, and so it is difficult to compare our value with others.

In treating calcite-type structures with a corner-linked model we ignore the carbonate group altogether, and hence do not take into account the motion of the CO_3 group with increasing temperature. The model does, however, allow us to gain some understanding of the thermal expansion along **c**, i.e., slight opening of the linkage and concomitant expansion of the octahedra, with the latter being the more important mode.

As pointed out previously, calcite is one of the few inorganic solids with negative thermal expansion along an axis. Megaw (1970) formulated an explanation for this feature through a general analysis of the thermal ellipsoids. Unfortunately her model predicts negative thermal expansion along **a** for all calcite-type structures. Ramachandran and Srinivasan (1972) have presented an excellent discussion of the role of Poisson contraction in calcite. Through analysis of the room temperature second and third order elastic constants, they show that vibrations of normal modes parallel to the unique axis will have higher frequencies than those perpendicular to it. Hence, as the crystal is heated, vibrations parallel to the three-fold axis gain more energy, and expansion is greater in this direction. Since the amount of the Poisson contraction depends on the amount of expansion, we can see that a large contraction may (although not necessarily) correspond to a strong expansion. Unfortunately the higher-order elastic constants of magnesite are not available.

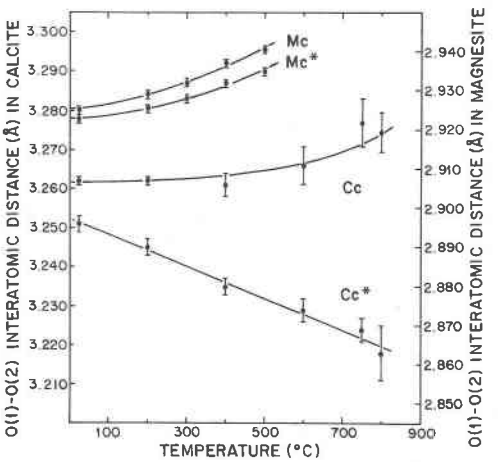

Fig. 7. Variation of the O(1)–O(2) interatomic distance with increasing temperature for calcite and magnesite. Abbreviations: Cc = calcite; Cc* = calcite, calculated from libration-corrected positions.

The negative thermal expansion of the *a* cell edge in calcite is best explained through the relatively large (when compared with magnesite) libration of the CO_3 group about the three-fold axis. One way to illustrate the effect of libration is through the use of the libration-corrected position of oxygen.[3] Of particular interest is the basal octahedral edge length O(1)–O(2), since it lies within {00.1}. The trend is shown in Figure 7. We hasten to point out that the O(1)–O(2) interatomic distance calculated from corrected oxygen positions is itself *not* corrected for libration. Such a correction would be invalid since there is no rigid-body motion *between* CO_3 groups, but only *within* them. For magnesite the values for both uncorrected and corrected oxygen positions increase with temperature, the former at a slightly faster rate. In contrast the corresponding values in calcite diverge with increasing temperature; the uncorrected values increase as in magnesite, whereas the corrected values decrease. The latter indicates a net contraction of the basal edge of the octahedra, thus yielding negative expansion along **a**. A similar analysis of the lateral edge (O(1)–O(6)) of the CaO_6 octahedron shows positive expansion throughout.

The nature of the $(Ca,Mg)CO_3$ solid solution is one of the most interesting problems in carbonate crystal chemistry. Opposite thermal expansion coefficients in calcite and magnesite lead to the question of what happens to the thermal expansion of *a* in a magnesian calcite, i.e., at what Ca/Mg ratio does the negative thermal expansion of **a** become positive, much in the manner of the keatite solid solution (Li, 1973). Simple high-temperature powder dif-

[3] The libration correction to the C–O bond may be cast in terms of a corrected position of oxygen.

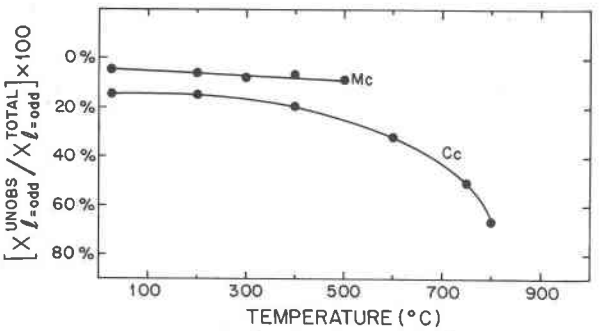

Fig. 8. Variation of the percentage of l = odd reflections unobserved with increasing temperature for calcite and magnesite. Abbreviations: $X^{unobs}_{l=odd}$ = number of l = odd reflections unobserved ($I < 2\sigma_I$); $X^{total}_{l=odd}$ = number of l = odd reflections total.

fraction experiments would answer this interesting question.

Speculations on phase transition

Several investigators, utilizing a variety of techniques, have found evidence for one, possibly two, phase transitions in calcite at high temperatures (800–1000°C) (cf. Reeder, 1983; Carlson 1983). No discussion is given for the proposed calcite–$CaCO_3$ V transition since we do not have crystallographic data in that temperature range. This phase transition has been compared with that in the isostructural $NaNO_3$. Neutron diffraction experiments (Paul and Pryor, 1971) have shown that sodium nitrate undergoes a transition from $R\bar{3}c$ to $R\bar{3}m$, apparently involving rotational disorder of the NO_3 groups. Other workers have examined the structure with X-ray analysis (Strømme, 1969; Terauchi and Yamada, 1972). However, it would be of more than pedantic interest to see this structure refined in a manner similar to that done here (i.e., TLS and anisotropic refinements).

Mirwald (1976, 1979a,b) has presented evidence for a phase transition in calcite at approximately 800°C, the calcite–$CaCO_3$ IV transition. Our data show no anomalies at 800°C; the structure refines to an acceptable residual in space group $R\bar{3}c$. Fourier maps reveal no extra peaks; specifically, no evidence is found for any occupancy of oxygen in the "disordered" position. Mirwald (1979b) has also found a reversal in the negative thermal expansion of a and an increase in the expansion of the c cell edge. The MTEC for a in this study remains negative up to 900°C. It should be pointed out that although a change in the sign of thermal expansion often marks a phase transition, it does not require one. Several compounds go from a negative expansion to positive without a phase transition.

Chang (1965), Tsuboi (1927), and Mirwald (1979b) have discussed the intensity decrease of the $11\bar{2}3$ reflection in calcite with increased temperature. They describe a marked decrease at about 700°C. We find an interesting trend in the l = odd reflections in calcite. Reflections that obey the rule l = odd derive most of their intensity from oxygen scattering. With increasing temperature we find that these reflections disappear preferentially over reflections where l = even (Fig. 8). By "disappear" we mean that they become statistically unobserved within $I < 2\sigma_I$. While this has been interpreted as a precursor to the proposed phase transition from calcite–$CaCO_3$ V at 1000°C, it is more likely that this is a result of increased thermal vibration. It should be noted that this trend is not observed in the magnesite data.

In conclusion, our data question the existence of Mirwald's $CaCO_3$ IV phase. A possible precursor for the proposed $CaCO_3$ V transition is indicated, although the interpretation is speculative. Much more work needs to be done in this area before these interesting questions are resolved.

Acknowledgments

We wish to thank K. Baldwin and J. Prosky for assistance during the course of this study. Discussions with D. Swanson were very beneficial. We thank Howard Belsky for the magnesite crystals and Lois Annechini-Moore for typing. The manuscript was substantially improved through critical reviews by C. T. Prewitt, J. W. Downs, and L. W. Finger. One of us (SAM) wishes to thank the U.S. National Committee for Crystallography for a travel grant to present a report of this data at the XIIIth IUCr Congress in Germany.

Financial support was provided by NSF Grant EAR 8106629A01 (RJR).

References

Bayer, G. (1971) Thermal expansion anisotropy of dolomite-type borates, $Me^{2+}Me^{4+}B_2O_6$. Zeitschrift für Kristallographie, 133, 85–90.

Beals, R. J. and Cook, R. L. (1957) Directional dilation of crystal lattices at elevated temperatures. Journal of the American Ceramic Society, 40, 279–284.

Becker, P. J. and Coppens, P. (1975) Extinction within the limit of validity of the Darwin transfer equations. III. Non-spherical crystals and anisotropy of extinction. Acta Crystallographica, A31, 417–425.

Boeke, H. E. (1912) Die schmelzerscheinungen und die umkehrbare umwandlung des calcium carbonates. Neues Jahrbuch für Mineralogie Geologie, 1, 91–121.

Brown, G. E., Sueno, S., and Prewitt, C. T. (1973) A new single-crystal heater for the precession camera and four-circle diffractometer. American Mineralogist, 58, 698–704.

Burton, B. and Kikuchi, R. (1984) Thermodynamic analysis of the system $CaCO_3$–$MgCO_3$ in the tetrahedron approximation of the cluster variation method. American Mineralogist, 69, 165–175.

Busing, W. R. and Levy, H. A. (1964) The effect of thermal motion on the estimation of bond-lengths from diffraction measurements. Acta Crystallographica, 17, 142–146.

Cameron, M., Sueno, S., Prewitt, C. T., and Papike, J. J. (1973) High-temperature crystal chemistry of acmite, diopside, hedenbergite, jadeite, spodumene, and ureyite. American Mineralogist, 58, 594–638.

Carlson, W. D. (1980) The calcite–aragonite equilibrium: effects of Sr substitution and anion orientational disorder. American Mineralogist, 65, 1252–1262.

Carlson, W. D. (1983) The polymorphs of $CaCO_3$ and the aragonite-calcite transformation. In R. J. Reeder, Ed., Carbonates: Mineralogy and Chemistry, Reviews in Mineralogy, Vol. 11, p. 191–225. Mineralogical Society of America, Washington, D. C.

Chang, L. L. Y. (1965) Subsolidus phase relations in the systems $BaCO_3$-$SrCO_3$, $SrCO_3$–$CaCO_3$, and $BaCO_3$–$CaCO_3$. Journal of Geology, 73, 346–368.

Cherin, P., Hamilton, W. C., and Post, B. (1967) Position and thermal parameters of oxygen atoms in sodium nitrate. Acta Crystallographica, 23, 455–460.

Cohen, L. H. and Klement Jr., W. (1973) Determination of high-temperature transition in calcite to 5 kbar by differential thermal analysis in hydrostatic apparatus. Journal of Geology, 81, 724–727.

Effenberger, H., Mereiter, K., and Zemann, J. (1981) Crystal structure refinements of magnesite, calcite, rhodochrosite, siderite, smithsonite and dolomite with discussion of some aspects of the stereochemistry of calcite-type carbonates. Zeitschrift für Kristallographie, 156, 233–243.

Finger, L. W. (1975) Least-squares refinement of the rigid-body motion parameters of CO_3 in calcite and magnesite and correlation with lattice vibrations. Carnegie Institution of Washington Year Book, 74, 572–575.

Finger, L. W. and Prince, E. (1975) A system of FORTRAN IV computer programs for crystal structure computations. U.S. National Bureau of Standards Technical Note 854.

Gunderson, S. H. and Wenk, H.-R. (1981) Heterogeneous microstructures in oolitic carbonates. American Mineralogist, 66, 789–800.

Hazen, R. M. (1976) Effects of temperature and pressure on the cell dimensions and X-ray temperature factors of periclase. American Mineralogist, 61, 266–271.

Hazen, R. M. and Finger, L. W. (1982) Comparative Crystal Chemistry. John Wiley and Sons, New York.

Hazen, R. M. and Prewitt, C. T. (1977) Effects of temperature and pressure on interatomic distances in oxygen-based minerals. American Mineralogist, 62, 309–315.

Ibers, J. A. and Hamilton, W. C. eds. (1974) International Tables for X-ray Crystallography, Vol. 4. Revised and Supplementary Tables. Kynoch Press, Birmingham.

Isherwood, B. J. and James, J. A. (1976) Structural dependence of the optical birefringence of crystals of calcite and aragonite-type structures. Acta Crystallographica, A32, 340–341.

Krishna Rao, K. V., Nagender Naidu, S. V., and Satyanarayana Murthy, K. (1968) Precision lattice parameters and thermal expansion of calcite. Journal of Physics and Chemistry of Solids, 29, 245–248.

Lager, G. A. and Meagher, E. P. (1978) High-temperature structural study of six olivines. American Mineralogist, 63, 365–377.

Li, C. (1973) The role of lithium in stabilizing some high-temperature silica phases. Zeitschrift für Kristallographie, 138, 216–236.

Lo, B. W. N. (1973) The polarizabilities of planar nitrate, carbonate and borate anions in crystal. Journal of Physics and Chemistry of Solids, 34, 513–520.

Markgraf, S. A. and Reeder, R. J. (1984) High-temperature crystal chemistry of calcite and magnesite. IUCr XIIIth Congress , Collected Abstracts, 145.

Megaw, H. D. (1970) Thermal librations and a lattice mode in calcite and sodium nitrate. Acta Crystallographica, A26, 235–244.

Megaw, H. D. (1971) Crystal structures and thermal expansion. Materials Research Bulletin, 6, 1007–1018.

Mirwald, P. W. (1976) A differential thermal analysis study of the high-temperature polymorphism of calcite at high pressure. Contributions to Mineralogy and Petrology, 59, 33–40.

Mirwald, P. W. (1979a) Determination of a high-temperature transition of calcite at 800°C and one bar CO_2 pressure. Neues Jahrbuch für Mineralogie, Mönatshefte, 7, 309-315.

Mirwald, P. W. (1979b) The electrical conductivity of calcite between 300 and 1200°C at a CO_2 pressure of 40 bars. Physics and Chemistry of Minerals, 4, 291–297.

Narayanaswamy, P. K. (1947) Influence of temperature on the Raman spectra of crystals. Part I: Calcite. Proceedings of the Indian Academy of Sciences, 26A, 511–520.

Paul, G. L. and Pryor, A. W. (1971) The study of sodium nitrate by neutron diffraction. Acta Crystallographica, B27, 2700–2702.

Peterson, R. G., Ross, F. K., Gibbs, G. V., Chiari, G., Gupta, A., and Tossell, J. A. (1979) Electron density study of calcite. (abstr.) EOS, 60, 415.

Ramachandran, V. and Srinivasan, R. (1972) Generalized Grüneisen parameters of elastic waves in calcite and its thermal expansion. Journal of Physics and Chemistry of Solids, 33, 1921-1926.

Reeder, R. J. (1983) Crystal chemistry of the rhombohedral carbonates. In R. J. Reeder, Ed., Carbonates: Mineralogy and Chemistry, Reviews in Mineralogy, vol. 11, p. 1–47. Mineralogical Society of America, Washington, D. C.

Robinson, K., Gibbs, G. V., and Ribbe, P. H. (1971) Quadratic elongation: a quantitative measure of distortion in coordination polyhedra. Science, 172, 567–570.

Schomaker, V. and Trueblood, K. N. (1968) On the rigid-body motion of molecules in crystals. Acta Crystallographica, B24, 63–76.

Strømme, K. O. (1969) The crystal structure of sodium nitrate in the high-temperature phase. Acta Chemica Scandinavica, 23, 1616–1624.

Sueno, S., Cameron, M., Papike, J. J., and Prewitt, C. T. (1973) The high-temperature crystal chemistry of tremolite. American Mineralogist, 58, 649–664.

Terauchi, H. and Yamada, Y. (1972) X-ray study of phase transition in $NaNO_3$. Journal of the Physical Society of Japan, 33, 446–454.

Tsuboi, C. (1927) On the effect of temperature on the crystal structure of calcite. Proceeding of the Imperial Academy (Japan), 3, 17–18.

Willis, B. T. M. and Pryor, A. W. (1975) Thermal Vibrations in Crystallography. Cambridge University Press.

Zachariasen, W. H. (1967) A general theory of X-ray diffraction in crystals. Acta Crystallographica, 23, 558–564.

Manuscript received, August 1, 1984;
accepted for publication, January 7, 1985.